Supporting Information

Temperature-dependent assembly of two 3D $[BW_{12}O_{40}]^{5-}$-based coordination polymers with visible light driven photocatalytic properties

Xin-Xin Lu*[a], Yu-Hui Luo[a], Yan Xu[a] and Hong Zhang[a]

[a] *Institute of Polyoxometalate Chemistry, Department of Chemistry, Northeast Normal University, Changchun, Jilin 130024, P. R. China*

** E-mail: zhangh@nenu.edu.cn (H. Zhang)*

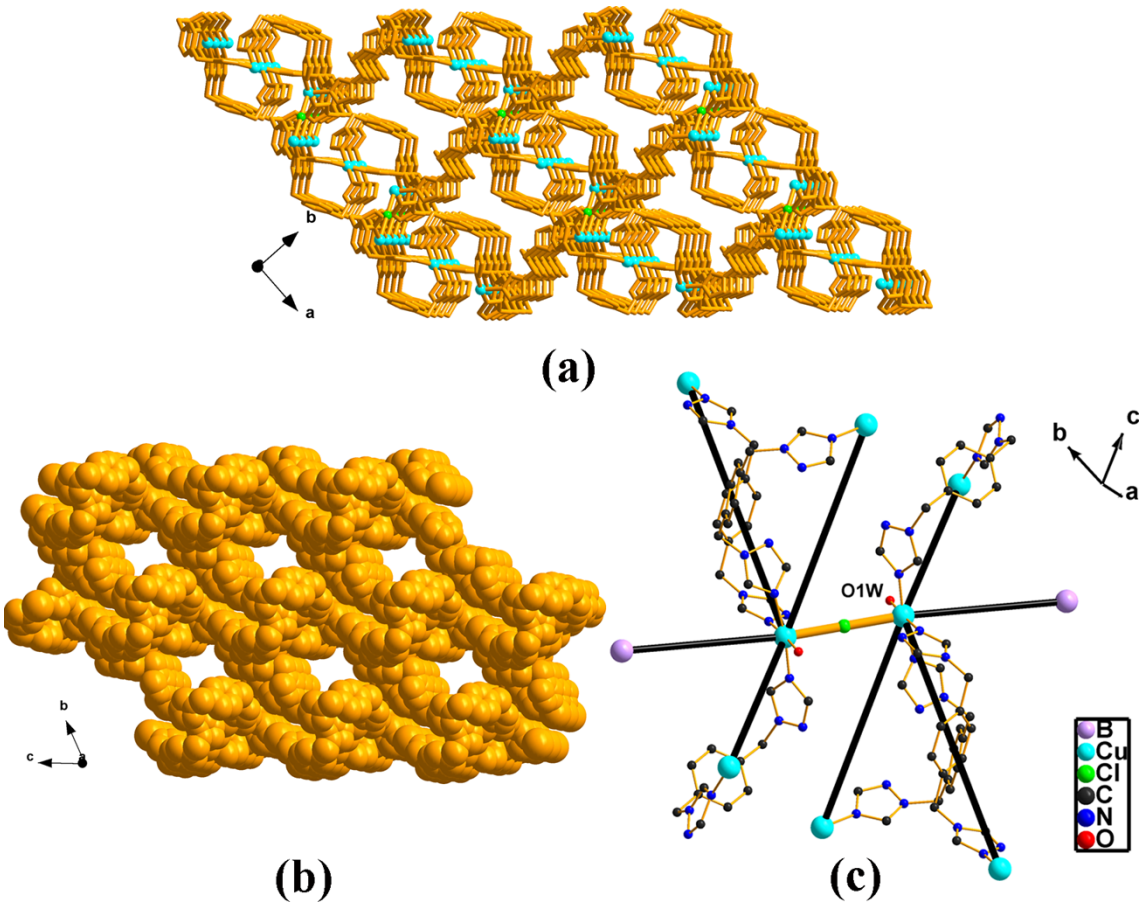

Fig. S1 (a) Cl atoms connect 2D layers to 3D main network. (b) Viewing along *a* axis, channels exist in host framework. (c) eight-connected node: Cu2-Cl-Cu2 as a node.

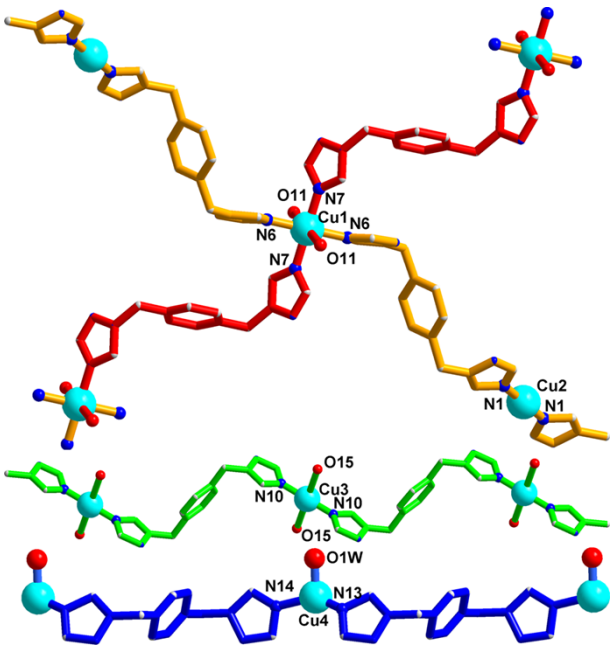

Fig. S2 Metal coordination and diverse chains in compound **2**.

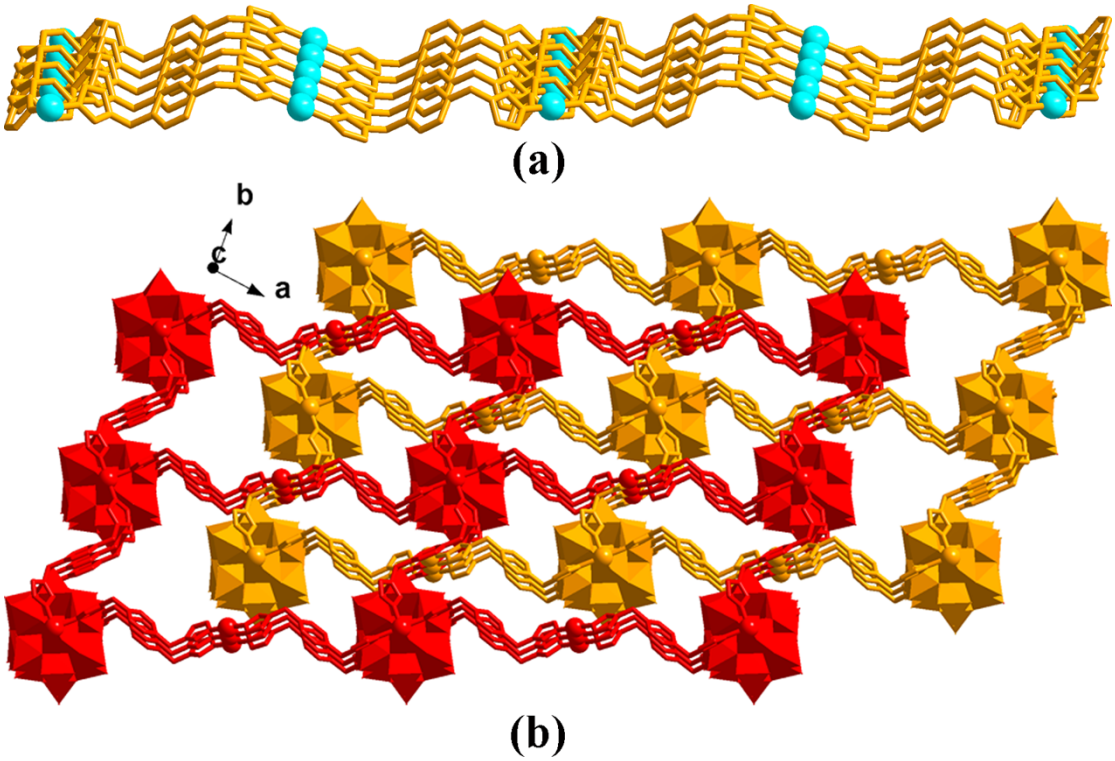

Fig. S3 (a) Cu1 and Cu2 atoms form 2D undulant layer. (b) POMs as linkages construct twofold interpenetrated networks.

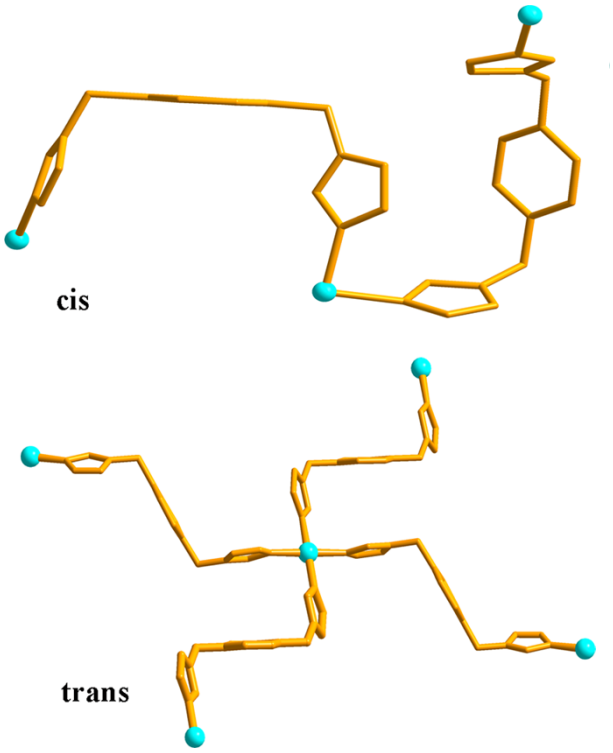

Fig. S4 All BBTZ ligands in compound **1** adopt cis-configuration, while trans-configuration in compound **2**.

The phase purity of compounds **1-2** was proved by using PXRD, the PXRD patterns of them were recorded at room temperature (Fig.S5 and S6). As shown in pictures, the peak positions of simulated and experimental patterns of compounds **1-2** are in agreement with each other, showing the good phase purity of them. The differences in intensity are due to the preferred orientations of the crystalline powder samples. The PXRD patterns of two compounds at the end of photocatalytic experiments are almost identical with that of the as-prepared sample.

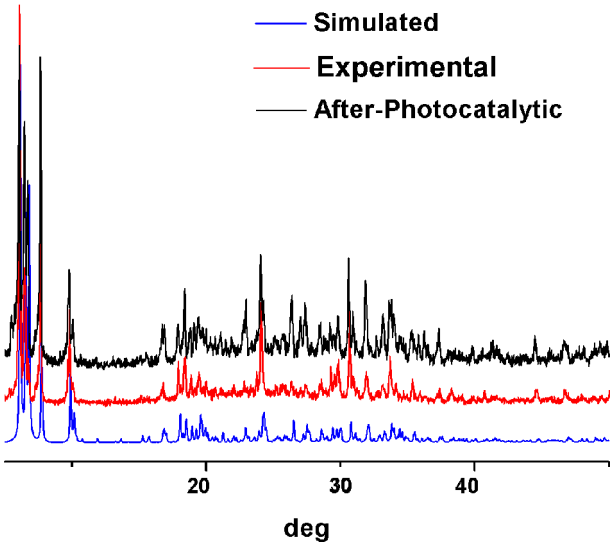

Fig. S5 XRD patterns of compound **1.**

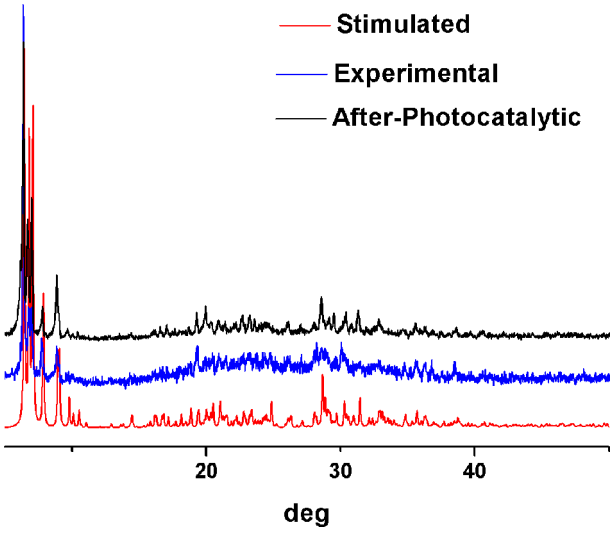

Fig. S6 XRD patterns of compound **2.**

In the IR spectrums of compounds **1** and **2** (Fig. S7 and S8), four characteristic peaks of $[BW_{12}O_{40}]^{5-}$ are observed in the range of 1000-700 cm. The peaks at 999, 951, 894, and 798 cm are ascribed to the vibrations of *v*(B-O), *v*(W=Od) and *v*(W–Ob/c–W), respectively. 3112(3128) cm are attributed to the vibrations of the *v*(C-H) in phenyl and pyridyl rings of BBTZ ligand. Peaks in the regions of 1649-1425cm may belong to the vibrations of the *v*(C=C), *v*(C=N) and *v*(C=N) in phenyl and triazole rings of BBTZ ligands in **1-2**. The peaks at ca. 3431 cm are attributed to the vibrations of *v*(H_2O).

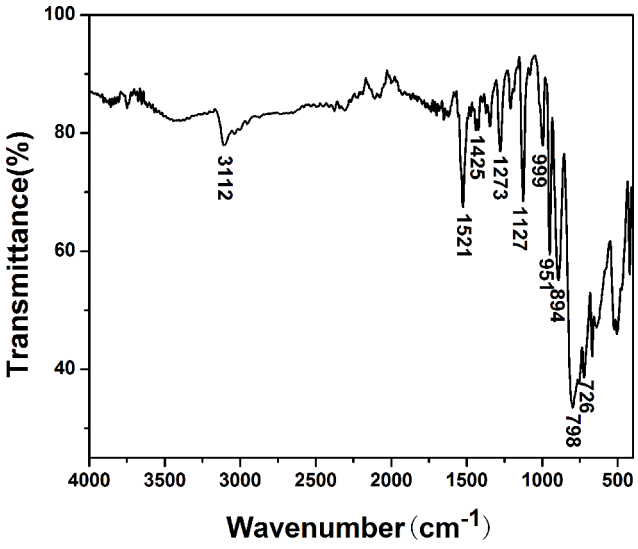

Fig. S7 IR spectrum of compound **1.**

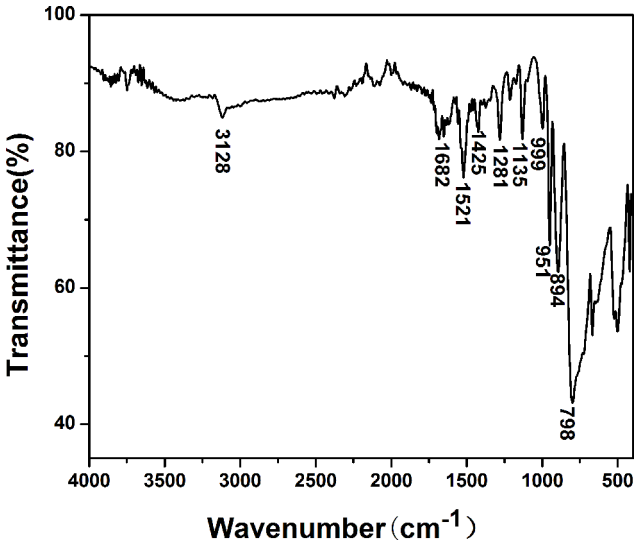

Fig. S8 IR spectrum of compound **2.**

Thermal stability of compounds **1**–**2** has been investigated by means of TG analysis (Fig.S9 and S10). The TG curve of compound **1** displays the first weight loss of 2.68% in the temperature range of 20~150 ℃, corresponding to two coordinated water molecules and six water molecules (calculated value 3.25%) . Further heating the framework goes on decomposing till about 300 ℃. Compound **2** is stable up to approximately 300 ℃, the dissociative and coordination water molecules lose before network resolving. But because of very small percentage, TG curve does not come out.

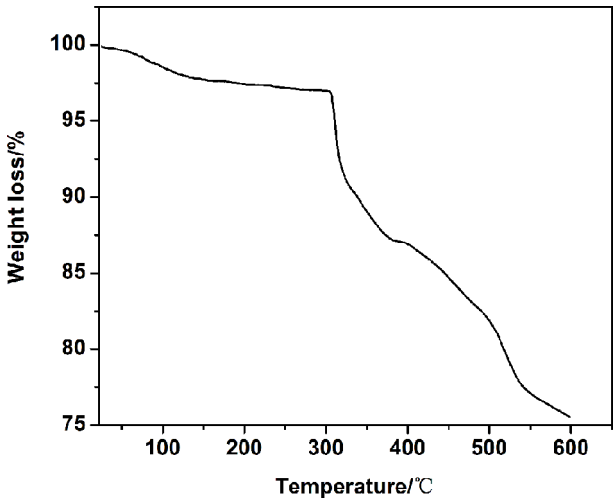

Fig. S9 TG curve of compound **1.**

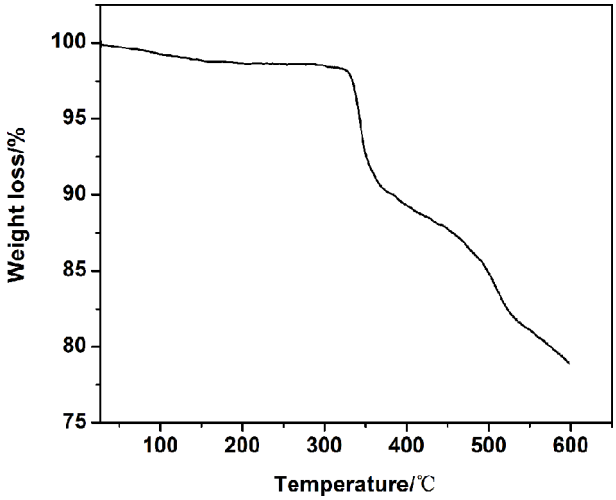

Fig. S10 TG curve of compound **2.**

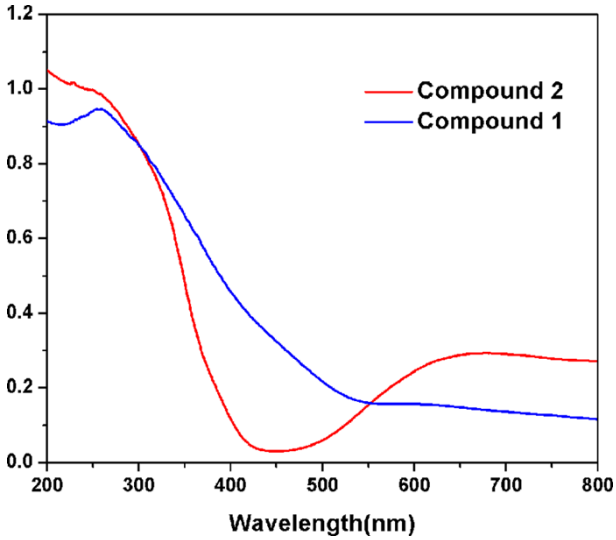

Fig. S11 The solid-state UV−vis spectra of compounds**.**

Photocatalytic Experiments

The experiment with a typical process, 30 mg of **1** or **2** was added in 350 mL

RhB solutions (5×10^{-5}mol L^{-1}) and then the solutions were magnetically stirred in the dark for 30 min. The mixture was then exposed to UV or visible light irradiation under stirring continuously, and 2.0 mL of solution was withdrawn regularly from the reactor for analysis. When performing visible photocatalysis experimental, 15 mmol of hydrogen peroxide solution (H_2O_2 30%) were added into the reaction solution. The photocatalytic activities were monitored by UV–vis measurements of the absorbency of the solution with a Cary 500 UV-Vis-NIR Spectrophotometer after given time intervals. The degradation rate of RhB solution was calculated by the following formula:

$$D = (A_0 - A_1) / A_0 \times 100\%$$

Where D is degradation rate, A_0 and A_1 are the characteristic absorbency of RhB solutions in adsorption equilibrium before and after irradiation, respectively.

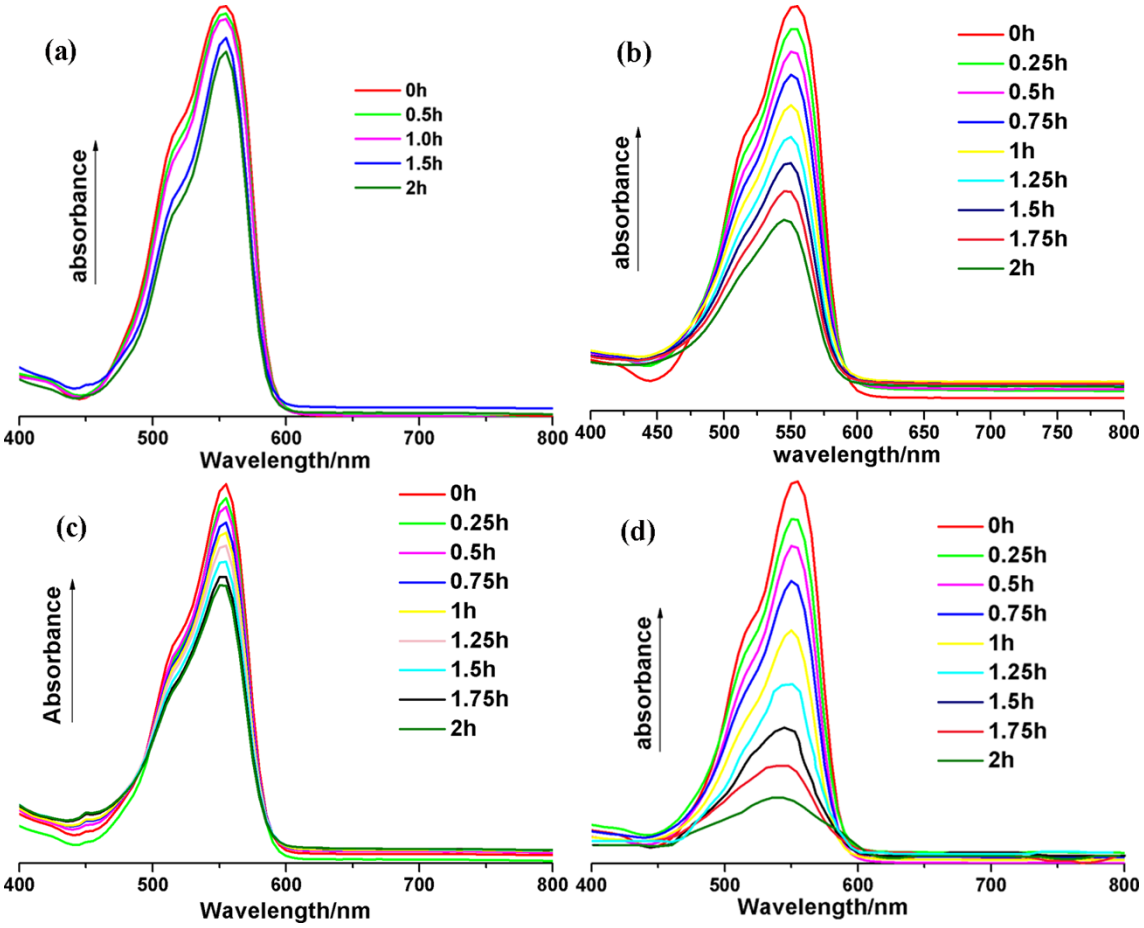

Fig. S12 Photodegradation of RhB under visible light irradiation: (a) only compound **1;** (b) compound **1** and 15mmol H_2O_2; (c) only compound **2**; (d) compound **2** and 15mmol H_2O_2.

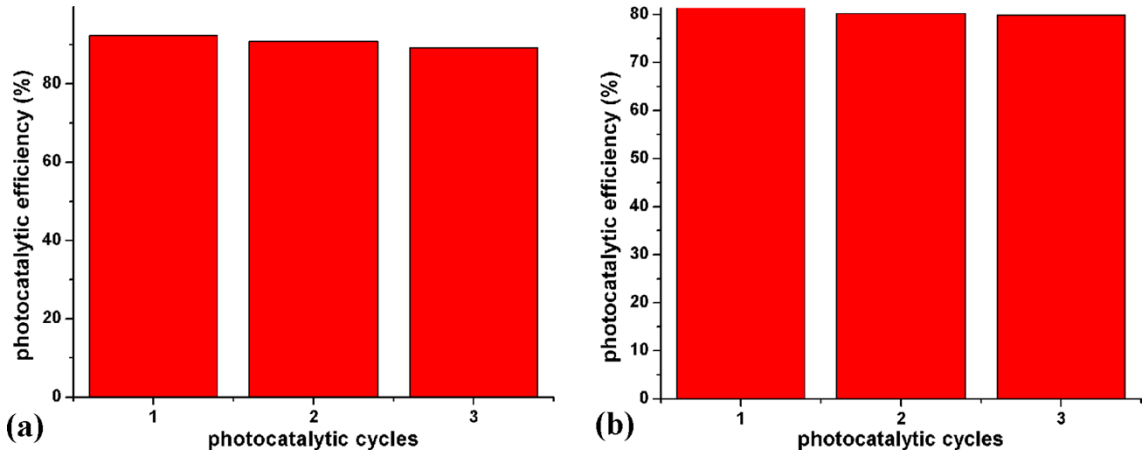

Fig. S13 (a) photocatalytic cycles efficiencies of compound **1** under ultraviolet light irradiation; (b) photocatalytic cycles efficiencies of compound **2** under visible light irradiation.

The N-heterocyclic BBTZ molecule has weak absorptions at 309nm and 410nm[1]. This characteristic makes the BBTZ molecule a suitable antenna to absorb effective light energy for the catalytic cluster[2], which will be beneficial for solar light utilization and photocatalytic efficiency enhancement. The UV-vis spectrum of compound **1** shows no absorption bands in the visible region, while for compound **2**, the spectrum shows obvious absorption from 400–800 nm (Fig. S11), which indicates the charge transfer between the metal–organic fragments and the POM in compound **2**.[3,4] RhB dye has strong absorption for visible light and its excited state has a rather low redox potential, which means that in our system the RhB dye itself can act as the sensitizer.[5] During the whole catalytic reaction process, two sensitizers coexist: the RhB dye and the Cu-BBTZ coordination fragments. A proposed photodegradation mechanism of organic dyes is that after excitation by visible light, the excited sensitizer injects electrons into the LUMO of the POM and these electrons are trapped by H_2O_2 to produce the oxidizing species $OH^{\cdot}$. Then, the radicals attack the organic substrates and degrade the dye (Scheme S1).[6-9]

When H_2O_2 is involved in the system, the following reaction will happen:

$$\text{POM-Cps} + H_2O_2 + H^+ \longrightarrow \text{Oxidized POM-CPs} + H_2O + {\cdot}OH$$

Thus, the H_2O_2 promote photocatalytic degradation of dyes.

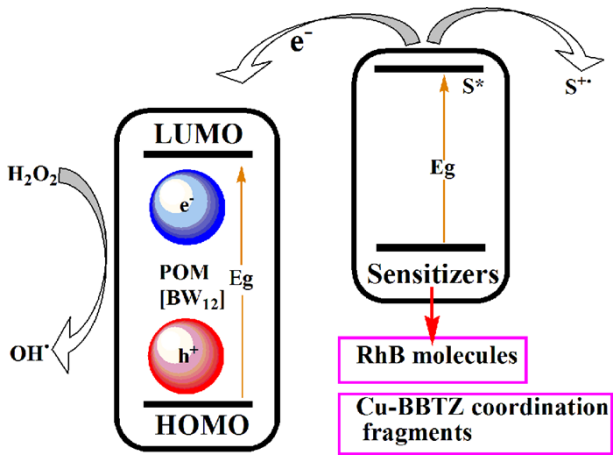

Scheme S1. Schematic diagram of the photocatalytic mechanism of compounds **1**-**2**.

The photocatalytic mechanism can refer to following papers:

1, X. Zhu, P. P. Sun, J. G. Ding, B. L. Li and H. Y. Li, *Cryst. Growth Des.*, 2012, 12, 3992-3997.

2, A. Hiskia, A. Mylonas and E. Papaconstantinou, *Chem. Soc. Rev.*, 2001, 30, 62–69.

3, H. X. Yang, T. F. Liu, M. N. Gao, H. F. Li, S. Y. Gao and R. Cao, *Chem. Commun.*, 2010, 46, 2429–2431.

4, L. Luo, H. S. Lin, L. Li, T. I. Smirnora and P. A. Maggard, *Inorg. Chem.*, 2014, 53, 3464 −3470.

5, T. Takizawa, T. Watanabe and K. Honda, *J. Phys. Chem.*, 1978, 82, 1391–1396.

6, T. Wen, D. X. Zhang and J. Zhang, *Inorg. Chem.*, 2013, 52, 12-14.

7, L. L. Wen, J. B. Zhao, K. Lv, Y. H. Wu, K. J. Deng, X. K. Leng and D. F. Li, *Cryst. Growth Des.*, 2012, 12, 1603-1612

8, Y. Q. Chen, G. R. Li, Y. K. Qu, Y. H. Zhang, K. H. He, Q. Gao and X. H. Bu, *Cryst. Growth Des.*, 2013, 13, 901-907

9, B. L. Fei, W. Li, J. H. Wang, Q. B. Liu, J. Y. Long, Y. G. Li, K. Z. Shao, Z. M. Su and W. Y. Sun, *Dalton Trans.*, 2014, 43, 10005.

Table S1. Selected bond lengths (Å) and angles (°) of compound **1**.

Cu(1)-O(3)	2.332(8)	N(12)-Cu(2)-O(1W)	90.9(5)
Cu(1)-N(1)	1.999(10)	N(13)-Cu(2)-N(14)	21.8(5)
Cu(1)-N(7)	1.980(11)	O(1W)-Cu(2)-N(14)	162.6(5)
Cu(2)-Cl(1)	2.609(18)	N(12)-Cu(2)-O(1)	79.2(4)
Cu(2)-N(12)	1.947(12)	N(12)-Cu(2)-N(6)#1	172.(6)
Cu(2)-N(13)	2.004(13)	N(13)-Cu(2)-N(6)#1	86.8(6)
Cu(2)-O(1W)	2.007(10)	O(1W)-Cu(2)-N(6)#1	92.0(6)
Cu(2)-N(6)#1	1.998(16)	N(7)-Cu(1)-O(3)#1	87.0(4)

Cu(2)-O(1)	2.497(10)	N(14)-Cu(2)-N(6)#1	93.9(6)
O(1W)#1-O(2W)#1	2.70(10)	O(1)-Cu(2)-N(6)#1	93.7(5)
O(2W)#1-O(4W)#1	2.70(10)	O(1W)-O(3WB)-O(4W)	98.0(7)
O(3WB)#1-O(4W)#1	3.029(6)	O(1W)-O(3WB)-O(2W)	52.9(9)
O(4W)#1-O(3WB)#2	2.880(6)	O(1W)-O(2W)-O(3WB)	52.9(8)
O(1W)#1-O(3WB)#1	2.70(10)	O(2W)-O(4W)-O(3WB)	72.3(4)
N(1)-Cu(1)-O(3)	88.7(4)	O(2W)-O(4W)-O(3WB)#2	93(2)
N(1)-Cu(1)-O(3)#1	91.3(4)	O(2W)-O(4W)-O(3WB)	72.3(14)
N(7)-Cu(1)-O(3)	93.0(4)	O(4W)-O(2W)-O(1W)	111.0(15)
N(7)-Cu(1)-O(3)#1	87.0(4)	O(4W)-O(2W)-O(3WB)	60.7(14)
N(7)#1-Cu(1)-N(1)	91.6(4)	O(4W)-O(3WB)-O(2W)	47.1(13)
N(7)-Cu(1)-N(1)	88.4(4)	O(4W)#2-O(3WB)-O(2W)	108.4(17)
N(12)-Cu(2)-N(13)	89.8(5)		

[a] Symmetry codes: #1, x, y, 1+z; #2, 1-x, 1-y, 2-z

Table S2. Selected bond lengths (Å) and angles (°) of compound **2**.

Cu(1)-N(6)	2.003(18)	N(7)#1-Cu(1)-N(7)	89.9(7)
Cu(1)-N(7)	1.968(17)	N(7)#1-Cu(1)-N(6)	89.9(7)
Cu(1)-O(11)	2.413(14)	N(7)#1-Cu(1)-O(11)	88.1(6)
Cu(2)-N(1)	1.873(18)	N(7)#1-Cu(1)-O(11)#1	91.9(6)
Cu(3)-N(10)	1.84(2)	N(1)-Cu(2)-N(1)#2	179.98
Cu(3)-O(15)	2.748(16)	N(10)#3-Cu(3)-O(15)#3	88.2(8)
Cu(4)-N(13)	1.7(4)	N(10)#3-Cu(3)-O(15)	91.8(8)
Cu(4)-N(14)	2.0(4)	N(13)-Cu(4)-N(14)#4	142(10)
Cu(4)-O(1W)	1.86(6)	O(1W)-Cu(4)-N(13)	105(10)
		O(1W)-Cu(4)-N(14)#4	104(9)

[a] Symmetry codes: #1, -x, -y, 1-z; #2, -2-x, -1-y, -z; #3, 1-x, -y, -z; #4=1-x, 1-y, 1-z.